Evaluating Instrumental Inhomogeneities in Global Radiosonde Upper Tropospheric Humidity Data Using Microwave Satellite Data

Isaac Moradi, Stefan A. Buehler, Viju O. John, Anthony Reale, and Ralph R. Ferraro

***Abstract*—In this paper, the overall quality of the water vapor profiles of global operational radiosonde data for the period 2000–2009 is investigated using upper tropospheric humidity (UTH) retrieved from microwave satellite data. Overall, the nighttime radiosonde data showed a dry bias (-5% to -15%) over Europe, Australia, and New Zealand and systematically moist bias (greater than 30%) over China and the former Soviet Union. The nighttime sonde data from the U.S. and Canada showed a bias between -10% and 20%. Most stations indicated a daytime radiation dry bias, except for a few stations from the U.S. and the former Soviet Union. A sensorwise comparison showed a large nighttime wet bias for the Russian (MRZ-3A and MARS) and Chinese GZZ-2 sensors, a relatively small nighttime wet bias for the U.S. Sippican and VIZ-B2 sensors, and a nighttime dry bias for the Chinese GTS1, Vaisala (RS80-A, RS80-H, RS90, RS92K, and RS92-SGP), and the U.S. VIZ-MKII sensors. All sensors had a daytime radiation dry bias, except for the Russian MRZ-3A sensor that had a daytime radiation wet bias that could be because of the daytime radiation bias correction. Because of the large differences between different radiosonde sensors, it is essential for UTH studies to only use the data measured using a single type of sensor at any given station.**

***Index Terms*—Microwave remote sensing (RS), radiosonde data, satellite data, tropospheric humidity, water vapor.**

Manuscript received April 13, 2012; revised August 14, 2012; accepted September 4, 2012. Date of publication November 16, 2012; date of current version May 16, 2013. The work of I. Moradi was supported by NOAA grant NA09NES4400006 (Cooperative Institute for Climate and Satellites) at the University of Maryland, Earth System Science Interdisciplinary Center (ESSIC). The work of I. Moradi, while working in Sweden, was supported in part by the Swedish Space Board under the project "Satellite Atmospheric Science" and in part by Lulea University of Technology. The work of V. John was supported in part by the Joint U.K. DECC/Defra Met Office Hadley Centre Climate Program under Grant GA01101 and in part by the U.K. Joint Weather and Climate Research Programme. The views, opinions, and findings contained in this paper are those of the authors and should not be construed as an official NOAA or U.S. Government position, policy, or decision.

I. Moradi is with the Earth System Science Interdisciplinary Center (ESSIC), University of Maryland, College Park, MD 20740 USA (e-mail: imoradi@umd.edu).

S. A. Buehler is with the Division of Space Technology, Department of Computer Science, Electrical and Space Engineering, Luleå University of Technology, SE-98128 Kiruna, Sweden (e-mail: sbuehler@ltu.se).

V. O. John is with the Met Office Hadley Centre, Exeter EX1 3PD, U.K. (e-mail: viju.john@metoffice.gov.uk).

A. Reale is with STAR, National Environmental Satellite, Data, and Information Service, National Oceanic and Atmospheric Administration, Camp Springs, MD 20746 USA (e-mail: tony.reale@noaa.gov).

R. R. Ferraro is with the Satellite Climate Studies Branch, STAR, National Environmental Satellite, Data, and Information Service, National Oceanic and Atmospheric Administration, College Park, MD 20740 USA (e-mail: ralph.r.ferraro@noaa.gov).

Color versions of one or more of the figures in this paper are available online at http://ieeexplore.ieee.org.

Digital Object Identifier 10.1109/TGRS.2012.2220551

I. Introduction

RADIOSONDE data have numerous applications in many areas of meteorology, climatology, and hydrology, such as validating satellite products [1]–[3], serving as *a priori* profiles for retrieving atmospheric profiles from satellite data [4], initializing weather forecast models [5], evaluating climatological features [6], [7], and assimilating into reanalyses [8]. Radiosonde data are prone to many errors, including sensor design, calibration, data processing, and contamination, particularly in the dry and cold conditions of upper troposphere [9]–[11]. A particular source of error is a dry bias owing to solar heating of the sensors [12], [13] that affects the data collected during daytime.

The quality of the radiosonde data can be investigated by the following: 1) comparing the data collected at neighboring stations, but this method does not work if both data sets have the same bias; 2) conducting intercomparison campaigns, e.g., [11], which is useful for characterizing the differences between various sensors but limited for evaluating global data, very expensive, and short term; and 3) comparison with independent data sets [14]–[18]. The latter is very useful to monitor the quality of operational data and does not need any extra measurements. This method can be applied in near real time. Data from, for instance, microwave [15] and infrared [16], [19] sensors aboard geostationary and polar-orbiting satellites and global positioning system radio occultation (RO) [14] can be used as the reference. In this paper, we use the satellite data measured by the microwave sensors aboard NOAA-15 to NOAA-18 and MetOp-A to evaluate the quality of the humidity profiles of global radiosonde data. We obtained the radiosonde data from the Integrated Global Radiosonde Archive (IGRA) developed by the National Climatic Data Center (NCDC) [20].

Soden and Lanzante [16] used the same approach to investigate the quality of operational radiosonde data (1979–1991) using satellite observations from 6.7-μm infrared sensors aboard TIROS-N and NOAA-6 to NOAA-11. They concluded that radiosonde data from the former Soviet Union, China, and eastern Europe show a systematically moist upper troposphere relative to satellite observations, whereas radiosonde data from the rest of the world show a systematically drier upper troposphere. Using one year of global radiosonde data, Moradi *et al.* [21] reported a wet bias over the former Soviet Union and China but a dry bias over the rest of the world. Sun *et al.* [14] used Constellation Observing System for Meteorology, Ionosphere, and Climate (COSMIC) RO profiles to investigate the quality of temperature and humidity profiles from 12 operational radiosonde types. They reported a dry bias for most sonde types which increases with altitude, except for Russian sensors which showed a moist bias of about 5%. They also compared the radiosonde simulated brightness temperatures (Tb's) with Tb's of microwave satellite data from MetOp-A and indicated that, for most sensors, except for Graw (Germany), Jin Yang (South Korea), and MRZ and MARS (Russia), sonde Tb's are greater than satellite Tb's. There is an inverse relation between the measured Tb's of water vapor channels and tropospheric humidity; therefore, greater sonde Tb's mean a dry bias for sonde data. Using COSMIC RO data from August to November 2006, Ho *et al.* [22] indicated a dry bias for Shang-E sensor (China) and a wet bias for VIZ sensor (USA). They reported that the MRZ sensor (Russia) and MEISEI (Japan) do not show any specific bias.

Here, we compare the upper tropospheric humidity (UTH) derived from radiosonde data with UTH retrieved from Advanced Microwave Sounding Unit-B (AMSU-B) and Microwave Humidity Sounder (MHS) observations. The aim is to evaluate the overall quality of the radiosonde humidity data in the upper troposphere. As the satellite data are also prone to errors and uncertainties, they cannot be taken as the absolute reference. However, previous studies show that satellite data have a good accuracy compared to the high-resolution high-quality radiosonde data. For example, Moradi *et al.* [1] compared satellite UTH with the nighttime high-resolution radiosonde data from the Atmospheric Radiation Measurement program measured using Vaisala RS92 sensors and reported that satellite data are always about 8%–12% (0.5–1.5 K) more moist than sonde UTH. It is worthwhile to mention that up to 0.5 K of this difference was attributed to the omission of ozone from the radiative transfer (RT) calculations.

Section II introduces the satellite and radiosonde data sets that were used for the comparison. Section III explains the method that was used to retrieve UTH from both satellite and sonde brightness temperatures. Results and discussions are in Section IV and Section V summarizes the comparison.

II. Satellite and Radiosonde Data

The AMSU-B is a cross-track scanning five-channel (16–20, channels 1–15 are of AMSU-A) microwave radiometer. The AMSU-B channels operate at 89.0, 150.0, 183.31 $\pm$ 1.00, 183.31 $\pm$ 3.00, and 183.31 $\pm$ 7.00 GHz. The instrument has a swath width of approximately 2300 km, with 90 scan positions. The AMSU-B footprint size, defined with respect to the half-power beamwidth, is approximately 15 km at nadir but increases toward the edge of the scan [23], [24]. The AMSU-B instruments are aboard the NOAA-15, NOAA-16, and NOAA-17 satellites, hereafter referred to as N15, N16, and N17, respectively. The MHS is aboard the NOAA-18, NOAA-19, and Metop-A satellites, hereafter referred to as N18, N19, and MA, respectively. MHS is very similar to AMSU-B, but the second channel has been moved to 157.0 GHz, and the fifth channel has only one passband at 190.311 GHz [24], [25]. In this paper, we used AMSU-B data from N15, N16, and N17 and MHS data from N18 and MA. The overall quality of the AMSU-B and MHS data is discussed, for example, in [26] and [1].

The IGRA project operated by the U.S. NCDC, National Oceanic and Atmospheric Administration, consists of radiosonde observations from around the world. According to Durre *et al.* [20] (see [20, Fig. 8]), about 65%–75% of the IGRA profiles reach 100 hPa, but just about 20%–30% reach 10 hPa. Therefore, we discarded radiosonde data above 100 hPa to maintain a homogeneous vertical extent. This introduces a bias of approximately 0.033–0.090 K, depending on the channel, with a small random error of 0.006–0.057 K [27]. AMSU-B/MHS water vapor channels are not normally very sensitive to altitudes above 100 hPa as their Jacobians peak at lower altitudes. Radiosonde profiles that do not contain data up to 100 hPa are not used in the study. Since 1958, the most frequent observation times are 00 : 00 and 12 : 00 Coordinated Universal Time (UTC), and most stations have two launches per day [20]. The original data set consists of data from over 1500 globally distributed stations. According to Sun *et al.* [14], who compared IGRA temperature and humidity data with COSMIC RO data, the overall difference between IGRA and COSMIC temperature profiles is 0.15 K, with a standard deviation of 1.5–2.0 K, throughout the troposphere and lower stratosphere. For more information about the IGRA data set, the reader is referred to [20]. Operational radiosonde data are normally reported at standard and significant pressure levels, but some profiles are only reported at the standard levels. In this paper, we only used radiosonde profiles that had both standard and significant levels. Buehler *et al.* [27] indicated that using low-resolution data with both standard and significant levels just introduces a small bias of 0.25% RH in the RT simulations relative to the high-resolution profiles. Obviously, interpolating low-resolution profiles without significant levels will introduce a large bias in the simulations and should be avoided. In addition, more than 200 stations in South America, Australia, India, China, and some other countries, may have continued reporting relative humidity as missing value in very cold conditions (below -40 °C) until 2006 [28]. These profiles, where any standard or significant levels were reported as missing, were excluded in our study. The U.S. stations stopped this convention before 2000 [28].

III. Methodology

We first simulated satellite brightness temperatures from radiosonde profiles. Then, we applied the same transformation method to both satellite and radiosonde Tb's to retrieve UTH. This approach avoids inconsistencies due to the varying vertical sampling of the satellites. The Atmospheric Radiative Transfer Simulator (ARTS) [29], [30] was used to simulate AMSU-B/MHS radiances from radiosonde profiles. The vertical profiles of air pressure, temperature, and water vapor volume mixing ratio were used as input to ARTS. Following Buehler and John [31], the following linear relationship was used to estimate UTH from the 183.31 $\pm$ 1.00 GHz radiances:

$$\ln(\mathrm{UTH}) = a + b \cdot Tb \tag{1}$$

where Tb is the radiance expressed in brightness temperature in kelvins and a and b are linear fit coefficients which are available separately for different viewing angles, so that radiances do not need to be limb corrected [32]. Microwave radiances are less sensitive to clouds than infrared radiances [33], but sufficiently optically thick ice clouds can affect microwave data [34]. A cloud filter explained in [35] and [36] was used to exclude cloud-affected pixels from the satellite data. The cloud filter works as follows. First, Channel 18 of AMSU is sensitive to higher altitudes of the troposphere than Channel 20. In clear-sky conditions, because of the natural lapse rate of air temperature, brightness temperatures of Channel 18 (Tb^{18}) are colder than brightness temperatures of Channel 20 (Tb^{20}). Ice clouds scatter outgoing radiation and reduce Tb^{20} more strongly than Tb^{18}. Therefore, in the presence of ice clouds, $\Delta Tb = Tb^{20} - Tb^{18}$, which is positive in clear-sky conditions, becomes negative. Second, ice clouds directly reduce the magnitude of Tb^{18}, so that, in the presence of ice clouds, Tb^{18} is less than a viewing-angle-dependent threshold $[T_{\mathrm{thr}}(\theta)]$. In summary, the conditions for clear-sky data are $\Delta Tb > 0$ and $Tb^{18} > T_{\mathrm{thr}}(\theta)$. Data not fulfilling either condition are considered cloud contaminated. T_{thr} for different viewing angles is given in [36].

A. Collocation Criteria

A radiosonde balloon typically drifts on average about 50 km horizontally while ascending from the ground to 100 hPa. Hence, the average Tb of a target area, rather than that of an individual pixel, is compared to the radiosonde-simulated radiance [27]. The target area is defined by a circle of radius 50 km from the launch site, which normally encompasses around 10–30 pixels. The pixels inside the target area have different viewing angles; hence, the radiosonde Tb's are simulated for the corresponding viewing angles.

The time difference between sonde launch time and satellite overpass time is very important for the collocations. Basically, sonde and satellite will be sampling different air masses, if the time difference is large. On average, a radiosonde takes about 20 min to reach 500 hPa and about 45–60 min to reach 200 hPa [1]. Therefore, for the collocation purpose, the radiosonde time is defined as its launch time plus 30 min. We limited the time difference between the satellite overpass and radiosonde time to 2 h. Most radiosondes are launched at 00 : 00 and 12 : 00 UTC, whereas satellites' overpass time is different at different stations. Consequently, the time difference criterion removes many collocations. The displacement of the sampled air masses during this time is also considered. Radiosonde wind data between 700 and 300 hPa, the altitude range most important for the humidity channels, are used to calculate the average wind vector. The average wind vector is multiplied by the time difference between the satellite overpass and radiosonde time. If the calculated displacement is greater than 50 km, the collocations are excluded.

In dry and cold conditions like winter at high latitudes, AMSU-B/MHS 183 $\pm$ 1 radiances are affected by the emitted radiance from the Earth's surface. In these cases, accurate surface emissivity data are required to simulate the outgoing radiation using RT models. We did not have access to such an accurate surface emissivity data set to estimate the surface contribution to the simulated radiances. Therefore, we limited our simulations to those profiles where the total precipitable water vapor was above 5 kg/m^2. In this case, the simulated radiance is not affected by the surface emissivity anymore even in very cold conditions [36].

B. Methodological Uncertainties

Methodological uncertainties, such as uncertainties in the satellite data, RT calculations, collocations, and sonde data, play an important role in this comparison; hence, different uncertainty sources are explained in detail in this section.

The sampling error, i.e., spatio-temporal difference between collocated satellite and sonde data, is one of the main error sources in this study. The relative sampling error, in humidity space, is estimated to be 3.3% per 3 h and 3.1% per 100 km in the troposphere (850–200 hPa) [14]. As we used 2 h and 50 km for the temporal and spatial thresholds, respectively, the sampling error is estimated to be about 3%, or less than 0.5 K.

The IGRA radiosonde data do not include ozone concentrations; therefore, radiances were calculated without the impact of ozone. The influence of this omission on calculated brightness temperatures of Channel 18 is less than 0.5 K, or approximately less than 3% RH dry bias [37].

We estimate that 0.5 K is also a reasonable approximation of the overall error of the RT model for this AMSU-B/MHS channel. This channel is close to the center of the 183.31-GHz water vapor line, so that uncertain continuum absorption parameters play only a very small role in the RT calculations. Large perturbations in the spectroscopic line parameters are necessary to cause significant radiance differences, which are unlikely given the well-established use of this line for atmospheric measurements. Altering water vapor spectroscopy data for the water vapor line near 183 GHz just introduces a small bias of less than 0.1 K in the RT calculations [1], [38]. The RT model ARTS itself has been validated against various other RT models [39], which leads to a rough estimate of the pure RT error (not including spectroscopic parameters) of less than 0.2 K. Since ARTS is a line-by-line RT model, it is generally expected that its calculations have better accuracy than fast RT models such as Radiative Transfer for TIROS Operation Vertical Sounders (RTTOV) and Community Radiative Transfer Model (CRTM) [39].

Prelaunch specification for uncertainty in the microwave satellite data (water vapor channels), known as noise-equivalent temperature ($\mathrm{NE}\Delta T$), is about 0.5–1.0 K [23]. There are several sources that could contribute to the postlaunch uncertainty in the satellite data, including uncertainties in the calibration coefficients, geolocation, cross-polarization, and antenna pattern. However, previous studies, e.g., [1], [15], [26], and [27], show generally good consistency between different satellites for this particular channel with somewhat larger errors for N15 than for the other satellites due to a radio frequency interference problem of the AMSU-B sensor on that satellite.

There are other error sources, such as the bias resulting from discarding radiosonde data above 100 hPa in the RT calculations or interpolating radiosonde profiles with both standard and significant levels, but those errors are negligible. In summary,

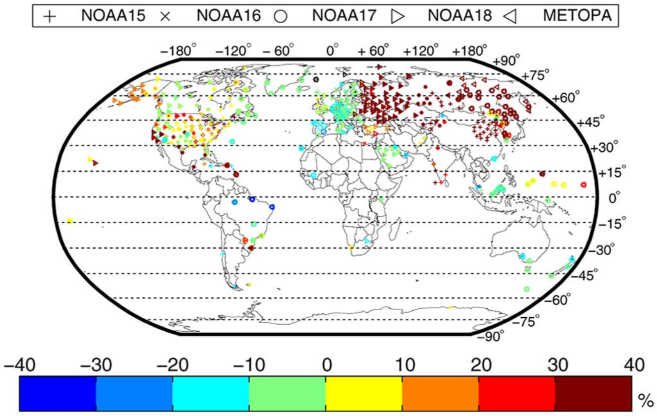

Fig. 1. Spatial distribution of the nighttime relative bias; sonde minus satellite. Sonde data have a wet bias over the former Soviet Union and China and a dry bias over Europe, Australia, and New Zealand. Most U.S. stations have a wet bias less than 20%; however, some of them have a wet bias greater than 30%.

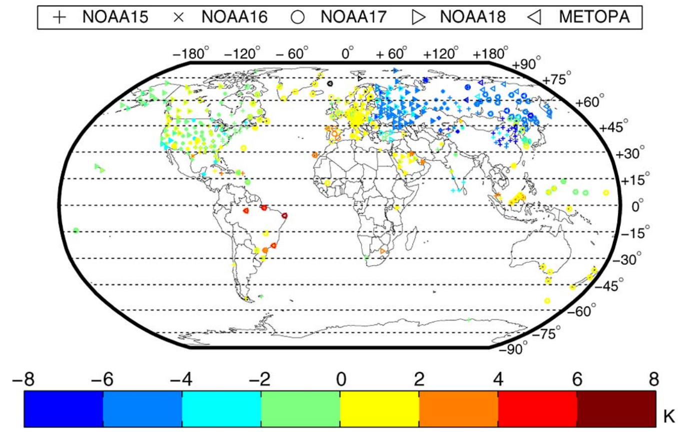

Fig. 2. Spatial distribution of the nighttime bias in terms of Tb in kelvins for the 183.31 $\pm$ 1 GHz water vapor channel. The bias is cold over China and the former Soviet Union (sonde Tb is less than satellite Tb) and warm over most other parts of the world.

our estimation is that the total methodological uncertainty is about 1–1.5 K that is mainly due to the omission of the ozone concentrations from the RT calculations, sampling error, RT model, and uncertainty in the satellite data.

IV. Results and Discussion

We compare sonde UTH versus satellite UTH, taking the satellite UTH as the reference. The well-known statistical parameters including relative bias (in percent and is calculated using UTH values), bias (in kelvins and is calculated using Tb values), and correlation coefficient between sonde and satellite UTH values are used for the comparison (see the Appendix for more details about the statistics). We limited the comparison to the stations with more than 50 collocated datapoints. The statistics are not reliable with fewer datapoints.

A. Nighttime Statistics

The spatial distribution of the nighttime relative bias for all the satellites is shown in Fig. 1. The values are averaged over the period 2000–2009. Note that, for some stations, these long-term averages are affected by sensor changes. The detailed discussion of biases for different sonde sensor types is given in Section IV-C. In total, 398 sonde stations are shown on the map. Therefore, more than two-thirds of the stations in the original data set are excluded from the comparison as they did not have good vertical resolution or enough collocated datapoints for comparison. Some stations are collocated with more than one satellite, so that 715 points are shown on the map. The main feature of the bias map is the country dependence of the bias resulting from the different sensor types that are used in different countries. Radiosonde data from the former Soviet Union overestimate UTH relative to the satellite data; sonde UTH is at least 20% greater than satellite UTH. This systematic error is related to the long response time of the Russian humidity sensors; the sensors are still responding to the lower altitudes, which are normally more moist than higher altitudes, while the balloon is ascending into the troposphere [16]. The relative bias over China is greater than 20% at most stations. Chinese stations that are equipped with the GTS1 sensors indicated a smaller wet bias than the stations that are equipped with the GZZ-2 sensors. The difference between these sensors is explained in Section IV-C.

Radiosonde data from Europe (including Scandinavian countries), Australia, and New Zealand showed a small dry bias. This is because these stations are equipped with Vaisala sensors; the dry bias of Vaisala sensors is already reported in [40] and [41]. The good agreement between sonde and satellite UTH values over Norway, Sweden, Finland, and Iceland shows that the large bias over Russia is not impacted by the Arctic cold weather. This confirms that the methodology, including the filters, is reliable even at high latitudes. Most Canadian stations have a relative bias less than 10% that can be either negative or positive. This bias is about 1 K in terms of Tb, which is estimated to be very close to the methodological uncertainty (see Section III-B for information about the methodological uncertainties).

The U.S. stations exhibit a large inhomogeneity that comes from the instrumentation. The U.S. data measured using Vaisala, Sippican, and VIZ-MKII sensors have a bias less than 5%, with a wet bias for Sippican and a dry bias for Vaisala and VIZ-MKII sensors. On the other hand, VIZ-B2 data show a large wet bias (about 16%) (for more details about the differences between the sensors, see Section IV-C).

Map of the nighttime bias in terms of Tb in kelvins is shown in Fig. 2. This is useful for remote sensing (RS) applications as RS communities normally deal with Tb rather than UTH. The bias in terms of Tb ranges from -6 to 6 K. Sonde data from the former Soviet Union and China have a cold bias (wet bias in terms of humidity) from -2 to -6 K. The bias over the U.S. ranges from -4 to 2 K. As we explained, this inhomogeneity over the U.S. is related to the different sensor types that are used in the United States. Data measured using Vaisala, and VIZ-MKII data have a warm bias, but VIZ-B2 data have a cold bias. Sippican has a negligible bias in terms of Tb (see Table II). The bias over Canada ranges from -2 to 1 K. Most European stations have a bias between 0 and 2 K.

The statistical parameters are consistent between different satellites, if the sonde data of a given station are collocated with more than one satellite. In most cases, the difference

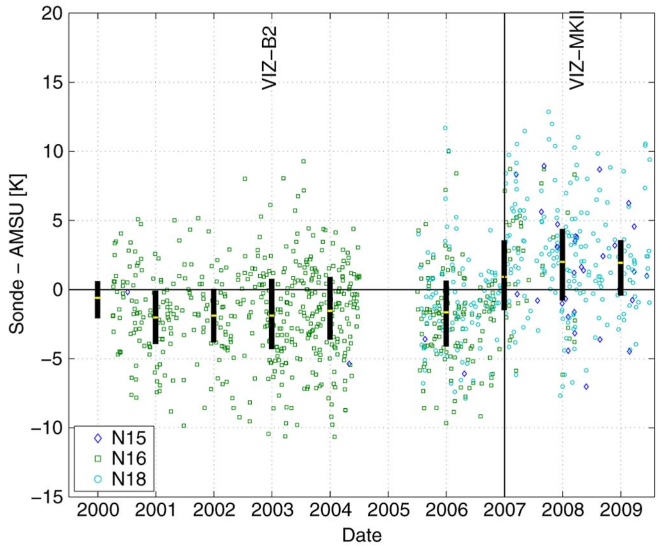

Fig. 3. Time series of the differences between collocated satellite and sonde Tb's at the station 72694 (Salem, U.S.). The sonde sensor was changed in July 2007 from VIZ-B2 to VIZ-MKII. Most N16 data are collocated with VIZ-B2 that has a cold bias, but N18 data are collocated with VIZ-MKII that has a wet bias. The vertical boxes show the 25th and 75th percentiles for each year, and the central yellow boxes show the annual mean.

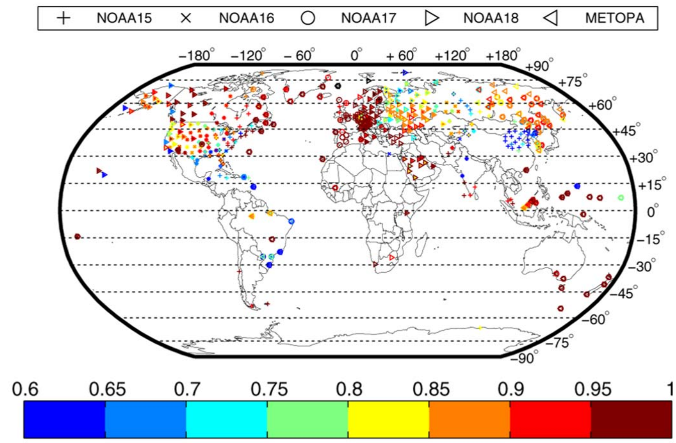

Fig. 4. Spatial distribution of the nighttime correlation coefficients in humidity space. The corrections are higher over Europe, Australia, New Zealand, and Canada than other parts of the world.

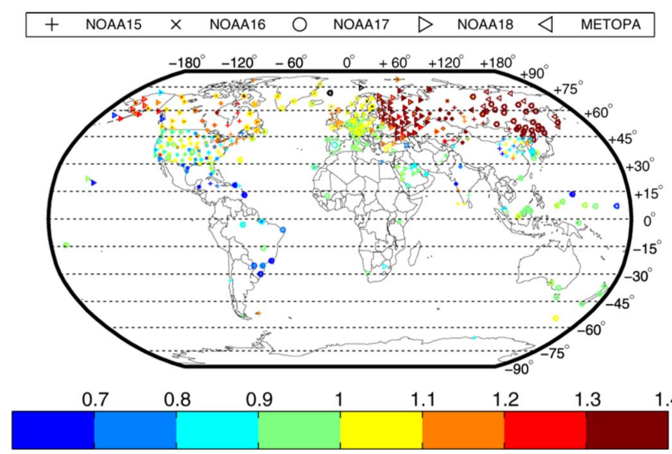

Fig. 5. Spatial distribution of the slope of the fitted line between sonde and satellite UTH data. The values indicate change in the radiosonde UTH per each unit change in the satellite UTH. The inhomogeneity in slope is related to the sensor type.

is negligible and can be attributed to the methodological uncertainties. Nevertheless, there are a few stations where the statistics between different satellites are quite different. The reason for these inconsistencies is that, in these cases, data from different satellites are collocated with sonde data measured using different sensor types. If the sensors have different biases, then the statistics will show a difference that is related to the sensor type rather than the satellite data. For instance, sonde data measured at the U.S. station 72694 (Salem; 44.92° N, 123.02° W) are collocated with the satellite data from N16 and N18. This station has a cold bias (sonde Tb is less than satellite Tb) relative to N16 data and a warm bias relative to N18 data. Fig. 3 shows the time series of the differences between sonde data and satellite data. According to the metadata, this station changed the sensor type in July 2007 from VIZ-B2 to VIZ-MKII. The figure clearly shows that N16 data are mostly collocated with VIZ-B2 data and N18 data are mostly collocated with VIZ-MKII data. VIZ-B2 has a cold bias, and VIZ-MKII has a warm bias relative to the satellite data (see Section IV-C). Therefore, the inconsistency between N16 and N18 is related to the sensor type rather than the satellite data.

The correlation coefficients between radiosonde and satellite UTH values are shown in Fig. 4. Sonde data from Europe, Australia, New Zealand, and Canada show a very significant correlation with the satellite data, above 0.9. Most U.S. and Russian stations have a correlation coefficient between 0.8 and 0.9. Other regions show a correlation between 0.6 and 0.8. The correlation coefficients over the U.S. are very inhomogeneous that is related to the different sensor types that are used in the U.S. network (see Section IV-C). High correlation coefficient and large bias, e.g., over Russia, mean that the bias is caused by a systematic error in the data. In the case of Russian data, this systematic error is due to the long response time of the sonde sensors.

Fig. 5 shows the global distribution of the slope of the fitted line, the linear regression between radiosonde UTH as the dependent variable and satellite UTH as the independent variable. In this comparison, the slope equals the change in the radiosonde UTH for each unit change in the satellite UTH. A slope of unity indicates a perfect match on average. Overall, the slope ranges from 0.6 to 1.41. The slope is greater than 1.2 over the former Soviet Union. This is because both Russian sensors have a slope greater than one (see Section IV-C). Some Chinese stations have a slope slightly greater than one, and some others have a slope less than 0.9. This is because GTS1 has a slope greater than one and GZZ-2 has a slope less than one. Most stations from Europe, Australia, and New Zealand have a slope close to unity, between 0.9 and 1.1. These stations are equipped with Vaisala sensors. RS80-A has a slope slightly less than one, but RS80-H has a slope slightly greater than one. Other Vaisala sensors, RS92 and RS90, have a slope very close to one. There is a large inhomogeneity over the U.S. that is related to the sensor type. All U.S. sensors (Sippican, VIZ-B2, and VIZ-MKII) have a slope less than one (see Fig. 8), but other sensors used in the U.S., such as RS80-H, have a slope slightly greater

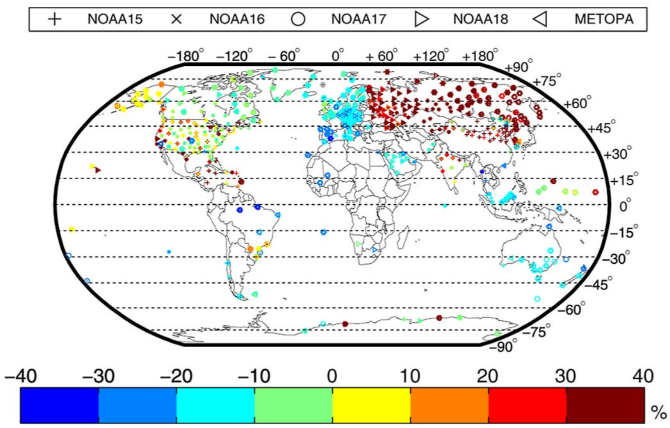

Fig. 6. Spatial distribution of the daytime relative bias. Over Europe, Australia, and New Zealand, the daytime bias is greater than the nighttime bias that is caused by the daytime radiation dry bias.

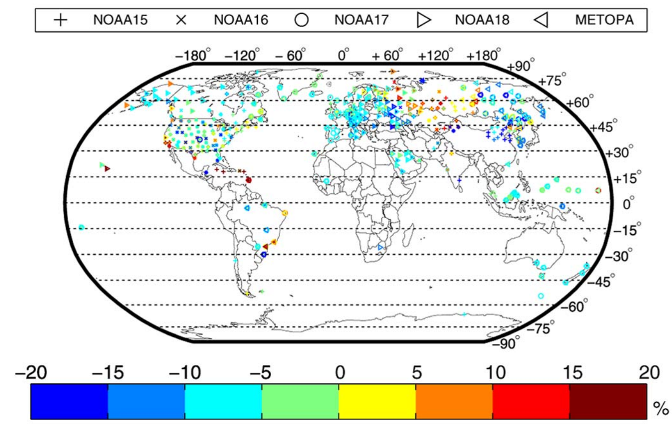

Fig. 7. Daytime radiation bias in percent (daytime minus nighttime relative bias). Most parts of the world have a daytime radiation dry bias, except for a few stations from North and South America and some stations from the former Soviet Union.

than one. Most Canadian stations have a slope between 1 and 1.2, but a few of them have a slope greater than 1.2.

The best agreement between sonde and satellite UTH values is where the absolute bias is small, the slope is close to unity, and the correlation coefficient is very significant. Therefore, data from most European stations, Australia, New Zealand, most Canadian stations, and also some stations from the U.S. show good agreement with the satellite data. Our findings are consistent with Soden and Lanzante [16] who reported a wet bias over the former Soviet Union, China, and eastern Europe and a dry bias over the rest of the globe. However, unlike Soden and Lanzante [16], we found a small dry bias over eastern Europe. The reason is that, in recent years, those countries have replaced Russian sensors with Vaisala sensors.

B. Daytime Statistics

The global distribution of daytime relative bias is shown in Fig. 6. Overall, Russian and Chinese sonde data have a daytime wet bias greater than 20%. The bias over Europe, Australia, and New Zealand is between 0% and −30%. Most Canadian stations have a dry bias less than 20%, but a few of them show a small wet bias. Some Canadian stations have a small wet bias with one satellite and small dry bias with the other satellite(s). As we explained before, these biases are in the range of the methodological uncertainty. Therefore, we can conclude that the Canadian stations have a small bias that cannot accurately be identified as a wet or dry bias using microwave satellite data. The daytime bias over the U.S. is very inhomogeneous and ranges from −20% to 20%; a few stations even have a bias greater than 20%. As we explained before, this is related to the different sensor types that are employed at the U.S. stations.

The global distribution of daytime radiation bias (daytime minus nighttime relative bias) is shown in Fig. 7. It is worthwhile to mention again that some countries, including Russia and China, and even some individual stations, correct daytime data for radiation bias. Therefore, at those stations, the daytime radiation bias shows the efficiency of the radiation bias correction rather than the sensor daytime radiation bias. Some of the correction algorithms are even implemented in the preprocessing software and are known as automatic solar radiation bias correction.

TABLE I
NIGHTTIME AND DAYTIME SONDE MINUS SATELLITE UTH IN RELATIVE UNIT FOR DIFFERENT SENSORS. B, R, AND N ARE RELATIVE BIAS, CORRELATION COEFFICIENT, AND NUMBER OF OBSERVATIONS, RESPECTIVELY. n STANDS FOR NIGHTTIME, AND d STANDS FOR DAYTIME

Sensor	Bn	Rn	Nn	Bd	Rd	Nd	Bd - Bn
GZZ-2	59.78	0.56	5822	51.23	0.58	13524	-8.55
GTS1	-1.00	0.68	2179	-3.72	0.61	4411	-2.72
MRZ-3A	46.07	0.71	3220	50.53	0.71	5949	4.46
MARS	50.08	0.86	219	37.08	0.74	343	-13.00
Sippican	2.66	0.77	349	-5.68	0.74	703	-8.34
VIZ-B2	15.81	0.78	28629	15.70	0.74	40263	-0.11
VIZ-MKII	-2.36	0.73	643	-4.64	0.71	1200	-2.28
RS80-A	-8.76	0.92	97	-13.23	0.94	193	-4.47
RS80-H	-4.89	0.90	650	-11.57	0.90	1282	-6.68
RS90	-4.92	0.92	537	-13.14	0.92	1598	-8.21
RS92K	-7.23	0.97	356	-14.14	0.97	1261	-6.91
RS92S	-6.53	0.97	1657	-13.98	0.96	4618	-7.45

Fig. 7 shows that most stations have a daytime radiation dry bias, except for a few stations from the U.S. and Brazil and most stations from central Russia that have a daytime radiation wet bias. The Russian stations with a daytime radiation wet bias are equipped with MRZ-3A (see Section IV-C). It is not clear if the wet bias of this sensor is because of the daytime bias correction or is related to the sensor itself. The only explanation for the daytime radiation wet bias over the U.S. is that the collocated day and night data are measured using different sensors, so that the wet bias indicates the difference between nighttime bias from one sensor and daytime bias from another sensor. This can happen when a station has changed the sensor type. This may be another reason for the daytime radiation wet bias over Central Russia.

C. Sensor Intercomparison

We classified all the collocated data based on the sonde sensor type to evaluate the sensors' bias. We used only those data where the metadata clearly indicate the sensor type. There are many cases where the metadata are not updated for many

TABLE II
NIGHTTIME AND DAYTIME SONDE MINUS SATELLITE Tb IN KELVINS FOR DIFFERENT SENSORS. B, R, U, AND N ARE BIAS IN KELVINS, CORRELATION COEFFICIENT, UNCERTAINTY IN THE BIAS IN KELVINS, AND NUMBER OF OBSERVATIONS, RESPECTIVELY. n STANDS FOR NIGHTTIME, AND d STANDS FOR DAYTIME

Sensor	Bn	Rn	Un	Nn	Bd	Rd	Ud	Nd	Bd - Bn
GZZ-2	-5.70	0.64	0.08	5822	-4.98	0.66	0.06	13524	0.72
GTS1	1.03	0.74	0.17	2179	1.60	0.70	0.12	4411	0.57
MRZ-3A	-4.91	0.78	0.10	3220	-5.40	0.79	0.07	5949	-0.49
MARS	-5.44	0.93	0.43	219	-4.03	0.81	0.31	343	1.41
Sippican	0.05	0.82	0.39	349	1.20	0.78	0.25	703	1.16
VIZ-B2	-1.24	0.77	0.04	28629	-1.24	0.75	0.04	40263	0.00
VIZ-MKII	1.10	0.77	0.31	643	1.52	0.74	0.23	1200	0.42
RS80-A	1.29	0.96	0.63	97	2.00	0.96	0.46	193	0.72
RS80-H	0.64	0.93	0.19	650	1.70	0.94	0.14	1282	1.05
RS90	0.74	0.94	0.26	537	1.99	0.94	0.15	1598	1.25
RS92K	1.04	0.97	0.34	356	2.11	0.98	0.18	1261	1.07
RS92S	0.94	0.98	0.18	1657	2.10	0.98	0.11	4618	1.16

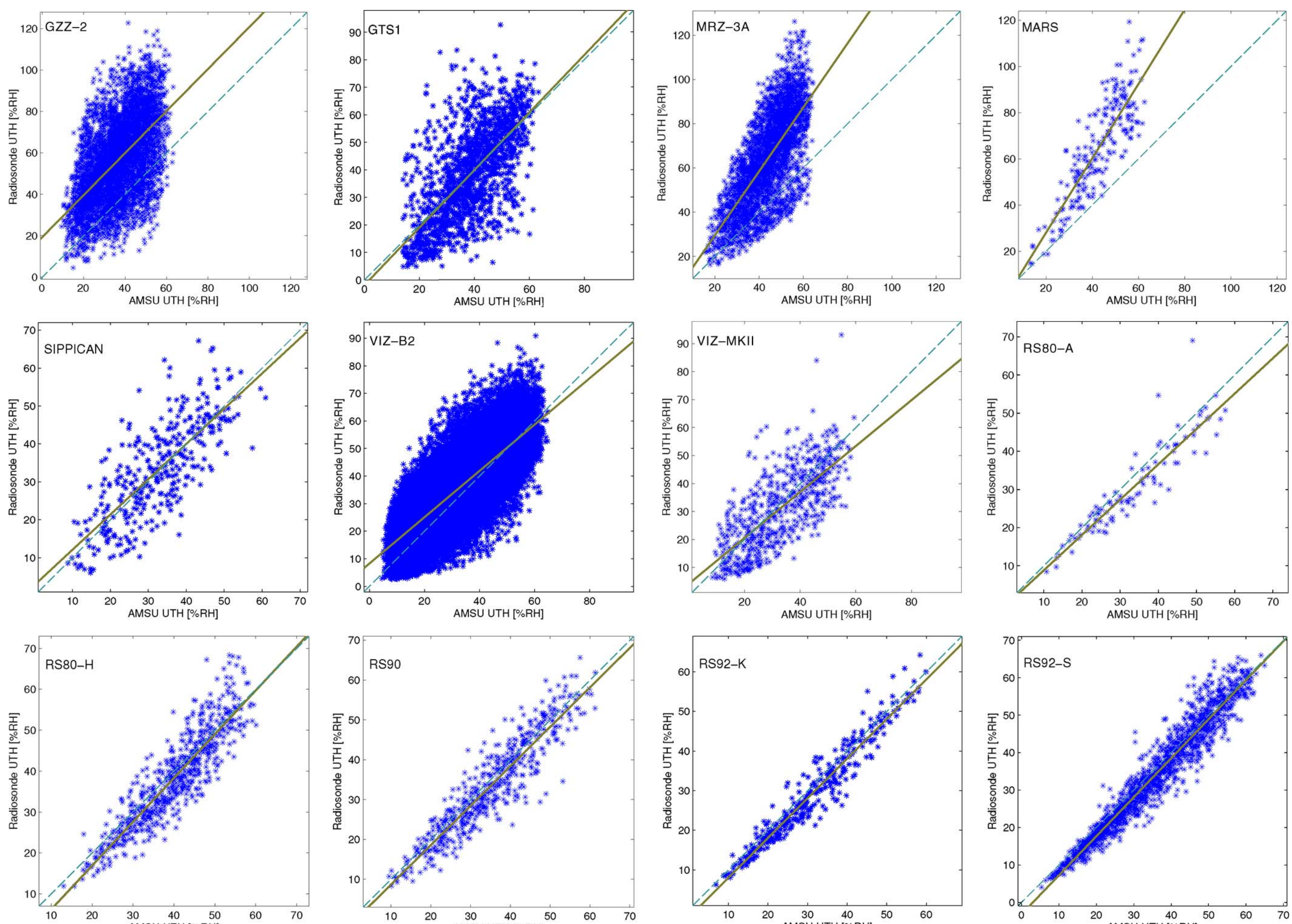

Fig. 8. Scatterplots of the nighttime sonde versus satellite UTH. The scatterplots show that Vaisala sensors have the best agreement with the satellite data.

years, and we cannot rely on the reported sensor type. We also excluded sensors that did not have enough collocated data. The day and night biases are separately shown in terms of UTH in Table I and in terms of Tb in Table II. The scatterplots for different sensors are shown in Fig. 8. The daytime and nighttime data are separated to see the daytime radiation bias. Some countries including Russia and China have an active radiation bias correction; therefore, at those stations, the day and night differences show the effectiveness of the radiation dry bias correction rather than the sensor daytime radiation bias. Chinese stations are mainly equipped with GZZ-2 403 MHz (GZZ-2) and GTS1 1680 MHz (GTS1) (see Table I). The nighttime bias for GZZ-2 is about 60% or -6 K. The new Chinese sensor (GTS1) has a small dry bias of about 1% or 1.0 K. However, GTS1 shows a large random bias and low correlation coefficient, which is related to the random bias of the temperature and humidity profiles in UT [11]. The GTS1 humidity sensor has a thin-film capacitor, like Vaisala sensors.

However, this kind of sensor can also give poor results if the manufacturer has not paid attention to the detail of the sounding system of the sensor, mounting, protective cap, and, also, the calibration of the humidity sensor at low temperatures [11]. Both Chinese sensors indicate a daytime radiation dry bias that is about 9% for GZZ-2 and about 3% for GTS1. The correlation coefficient is slightly higher for GTS1 than GZZ-2, 0.7 versus 0.6, respectively. The scatterplots, shown in Fig. 8, show that the bias of the Chinese sensors is not a function of UTH and their performance in the wet and dry conditions is the same.

The Russian sensors, MRZ-3A ARMA (MRZ-3A) and Russia/USSR MARS (MARS), showed a large wet bias, 46% (-4.9 K) and 50% (-5.4 K), respectively. These large biases are because of the long response time of the humidity sensor; the sensor is still responding to lower moist altitudes when ascending through the troposphere [16]. The correlation coefficient is more significant for MARS (0.9) than for MRZ-3A (0.7). The scatterplots, shown in Fig. 8, show that the wet bias of Russian sensors is a function of UTH and is greater in moist conditions than in dry conditions. The daytime radiation bias is wet for MRZ-3A (about 4.5% or -0.5 K) and dry for MARS (about -13% or 1.4 K). According to the IGRA metadata, most Russian stations have a daytime bias correction. Therefore, the differences between day and night biases do not indicate the sensors' radiation bias. This correction may be the reason for MRZ-3A daytime radiation wet bias.

We had enough collocated data for three U.S. sensors: SIPPICAN 1649-540 (Sippican), VIZ/Sippican B2 1492-540 (VIZ-B2), and VIZ/Sippican MKII (VIZ-MKII). Sippican indicated a negligible wet bias of about 2.7% or 0.1 K that is negligible compared to the methodological uncertainties. VIZ-B2 showed a wet bias of about 16% or -1.2 K. On the other hand, VIZ-MKII had a dry bias of -2.4% or 1.1 K. Daytime radiation dry bias was about -8% for Sippican, just 2% for VIZ-MKII, and negligible for VIZ-B2. The correlation coefficient for the U.S. sensors is about 70%–80% (see Tables I and II). VIZ-MKII data have the lowest correlation coefficient with the satellite data. The scatterplots, shown in Fig. 8, show that the mean bias for this sensor is low, but its measurements have large random errors which lead to lower correlation coefficients. In very cold conditions, as in the UT, the VIZ-MKII sensor stops responding to humidity at some point and continues to measure the same conditions as it ascends [41]. The low correlation coefficients of the other U.S. sensors, which are also from the random errors, might be introduced by the same issue.

Five different types of Vaisala sensors were identified and are reported in Tables I and II. These sensors are RS80-15 (RS80-A), RS80-15GH (RS80-H), Vaisala RS90 (RS90), Vaisala RS92K (RS92K), and RS92-SGP (RS92S). The common feature of the Vaisala sensors is that they have a dry bias of less than 10%, or less than 1 K. RS80-A has the largest nighttime bias of about 9% or 1.3 K. The smaller bias of RS90 than RS92 is not consistent with Miloshevich *et al.* [41] who reported a smaller dry bias for RS92 than RS90. Sun *et al.* [14] found a greater dry bias for RS90 and RS92 than RS80. We also found a greater dry bias for RS92 than RS80-H. However, we found a negligible difference between RS80-H and RS90 biases. In addition, our results show that RS80-A has the greatest bias among the Vaisala sensors. Our results are also consistent with Miloshevich *et al.* [10] who reported a greater dry bias for RS80-A than RS80-H. The large dry bias of RS80 sensors is because of the contamination of the capacitive-element humidity sensor by chemical substances, long-term instability of the sensor polymer, and time-lag error [10], [42]. The scatterplots, shown in Fig. 8, show that the Vaisala sensors have the best agreement with the satellite data. The dry bias of RS80-H is greater in dry conditions than in moist conditions, which is consistent with Buehler *et al.* [27]. Other Vaisala sensors perform similar in wet and dry conditions. During daytime, all the Vaisala sensors showed a larger dry bias in moist conditions than in dry conditions. Vaisala sensors have a daytime radiation dry bias ranging from 4.5% for RS80-A to 8.2% for RS90.

The uncertainties in kelvins are reported in Table II for both daytime and nighttime statistics. The uncertainty was calculated as $\mathrm{STD}/\sqrt{N}$, where STD is the standard deviation of the differences between sonde and satellite Tb's and N is the number of observations. We only calculated the uncertainties in terms of Tb, since the UTH values are in relative unit. As shown, in most cases, the uncertainties are less than 0.5 K. The uncertainty for the RS80-A nighttime bias is about 0.6 K that is affected by the low number of observations.

Overall, the results are broadly consistent with Sun *et al.* [14] but exhibit notable differences for some sensors. They reported a dry bias for most radiosonde types but a moist bias for the Russian MRZ and MARS sensors. Sun *et al.* [14] reported 5% moist bias for Russian sensors through the troposphere; we found a moist bias of about 50% for Russian sensors. They found a dry bias for the ShangE carbon hygristor (GTS1), 6% to 10% from 850 to 300 hPa; we found a smaller dry bias for this sensor, about 1% dry bias. It is worthwhile to mention that some sensors fail to respond to humidity changes in upper troposphere. According to our results and also previous studies, these sensors are Chinese GTS1 [43] and Sippican sensors [41], [44]. For example, the manufacturer specifications for the Sippican MarkIIa RH (VIZ-MKII) sensors are 5%–100% RH at temperatures above -50 °C, so that the measurements are not reliable in the cold upper troposphere conditions [41]. We also found a low correlation coefficient for GTS1, GZZ-2, Sippican, VIZ-B2, and VIZ-MKII. This is an indication that these sensors have a random error in the upper troposphere. This can be explained by the fact that these sensors fail to respond to humidity changes in cold conditions like in the upper troposphere.

V. Summary and Conclusion

We have evaluated the quality of UTH derived from ten years (2000–2009) of global operational radiosonde data versus UTH retrieved from microwave satellite data. Satellite data are prone to some errors and cannot be taken as the absolute reference. However, previous studies, e.g., [1], show that microwave satellite data just have a small bias compared to the high-resolution radiosonde data. Hence, they can be taken as a relative reference to evaluate the overall quality of other data sets. We found a large inconsistency between sonde data from different stations that can easily be explained by the sonde sensor type. The comparison showed that the Vaisala sensors, with a small dry bias, have the best agreement with the satellite data. Russian and Chinese sensors showed a large wet bias. The U.S. data exhibited a large inhomogeneity that is related to the different sensor types used in the U.S. VIZ-B2 showed a larger bias than Sippican and VIZ-MKII, 16% versus about 3%. On the other hand, VIZ-MKII showed a dry bias, but Sippican and VIZ-B2 indicated a wet bias. Most radiosonde types showed a daytime radiation dry bias, except for MRZ-3A. The MRZ-3A wet bias may be because of the daytime bias correction that is used in Russia. Our study shows that sonde data from most European countries, Australia, and New Zealand have better quality than sonde data from the rest of the globe. Because of the large differences between different radiosonde sensors, particularly in the upper troposphere, we propose to only use the sonde data measured using a single type of sensor for UTH studies in the upper troposphere. In addition, some radiosonde types, including VIZ-B2, Sippican, VIZ-MKII, GZZ-2, and GTS1, are not suitable for UT studies as they fail to respond to humidity changes in UT.

Appendix

The relative bias in percent is defined as the weighted mean of the relative differences between sonde and satellite UTH values

$$\text{Bias} = 100 \times \frac{\sum w_i \cdot \Delta D_i}{\sum w_i} \tag{2}$$

where $\Delta D_i = (\text{UTH}^{\text{sonde}} - \text{UTH}^{\text{sat}})/\text{UTH}^{\text{sat}}$ for the ith collocations and $w_i = 1/\sigma_i^2$, where σ_i is the standard deviation of the UTH of the pixels located inside the target area for the ith collocation.

The bias in kelvins is defined as the weighted mean of the differences between sonde and satellite brightness temperatures (Tb's)

$$\text{Bias} = \frac{\sum w_i \cdot \Delta B_i}{\sum w_i} \tag{3}$$

where $\Delta B_i = Tb^{\text{sonde}} - Tb^{\text{sat}}$ for the ith collocations and $w_i = 1/\sigma_i^2$, where σ_i is the standard deviation of the brightness temperature of the pixels located inside the target area for the ith collocation.

Acknowledgment

Radiosonde data were obtained from the Integrated Global Radiosonde Data archive sponsored by the National Oceanic and Atmospheric Administration (NOAA). The authors would like to thank ARTS radiative transfer community, many of whom have indirectly contributed by implementing features to the ARTS model. The authors would also like to thank D. E. Parker of the U.K. Met Office, for carefully reading this paper and his helpful comments, L. Neclos from the Comprehensive Large Array-data Stewardship System of the U.S. NOAA for providing the Advanced Microwave Sounding Unit data, and the anonymous reviewers for their valuable comments. This work contributes to European Cooperation in Science and Technology (COST) Action ES604 Water Vapor in the Climate System.

References

[1] I. Moradi, S. A. Buehler, V. O. John, and S. Eliasson, "Comparing upper tropospheric humidity data from microwave satellite instruments and tropical radiosondes," *J. Geophys. Res.*, vol. 115, p. D24 310, Dec. 2010.

[2] M. Martínez and M. Velázquez, "Evaluating layer precipitable water and lifted index from SEVIRI," *Proc. SPIE*, vol. 5571, pp. 116–126, 2004.

[3] S. Malmusi and M. Boccolari, "Upper and middle precipitable water calculated from METEOSAT-8/-9 tropospheric humidity and NCEP/NCAR temperatures," *Atmos. Res.*, vol. 95, no. 1, pp. 8–18, Jan. 2010.

[4] M. Schneider and F. Hase, "Optimal estimation of tropospheric H_2O and δD with IASI/METOP," *Atmos. Chem. Phys.*, vol. 11, no. 21, pp. 117207–11220, Nov. 2011.

[5] A. C. Lorenc, D. Barker, R. S. Bell, B. Macpherson, and A. J. Maycock, "On the use of radiosonde humidity observations in mid-latitude NWP," *Met. Atmos. Phys.*, vol. 60, no. 1–3, pp. 3–17, Mar. 1996.

[6] J. A. Añel, J. C. Antuña, L. de la Torre, J. M. Castanheira, and L. Gimeno, "Climatological features of global multiple tropopause events," *J. Geophys. Res.*, vol. 113, p. D00 B08, Nov. 2008.

[7] P. Ribera, C. Peña Ortiz, J. A. Añel, L. Gimeno, L. de la Torre, and D. Gallego, "Quasi-biennial modulation of the northern hemisphere tropopause height and temperature," *J. Geophys. Res.*, vol. 113, p. D00 B02, Jul. 2008.

[8] D. P. Dee, S. M. Uppala, A. J. Simmons, P. Berrisford, P. Poli, S. Kobayashi, U. Andrae, M. A. Balmaseda, G. Balsamo, and P. Bauer, "The ERA-Interim reanalysis: Configuration and performance of the data assimilation system," *Q. J. R. Meteorol. Soc.*, vol. 137, no. 656, pp. 553–597, Apr. 2011.

[9] W. P. Elliott and D. J. Gaffen, "On the utility of radiosonde humidity archives for climate studies," *Bull. Amer. Met. Soc.*, vol. 72, no. 10, pp. 1507–1520, Oct. 1991.

[10] L. M. Miloshevich, H. Vömel, A. Paukkunen, A. J. Heymsfield, and S. J. Oltmans, "Characterization and correction of relative humidity measurements from Vaisala RS80-A radiosondes at cold temperatures," *J. Atmos. Oceanic Technol.*, vol. 18, no. 2, pp. 135–156, Feb. 2001.

[11] J. Nash, T. Oakley, H. Vömel, and L. Wei, "WMO intercomparison of high quality radiosonde systems," World Meteorol. Org., Yangjiang, China, Tech. Rep., 2010.

[12] H. Vömel, H. Selkirk, L. Miloshevich, J. Valverde-Canossa, J. Valdes, E. Kyroe, R. Kivi, W. Stolz, G. Peng, and J. A. Diaz, "Radiation dry bias of the Vaisala RS92 humidity sensor," *J. Atmos. Oceanic Technol.*, vol. 24, no. 6, pp. 953–963, 2007.

[13] L. M. Miloshevich, H. Vömel, D. N. Whiteman, and T. Leblanc, "Accuracy assessment and correction of Vaisala RS92 radiosonde water vapor measurements," *J. Geophys. Res.*, vol. 114, no. D11, p. D11 305, Jun. 2009.

[14] B. Sun, A. Reale, D. J. Seidel, and D. C. Hunt, "Comparing radiosonde and COSMIC atmospheric profile data to quantify differences among radiosonde types and the effects of imperfect collocation on comparison statistics," *J. Geophys. Res.*, vol. 115, no. D23 104, 2010.

[15] V. O. John and S. A. Buehler, "Comparison of microwave satellite humidity data and radiosonde profiles: A survey of European stations," *Atmos. Chem. Phys.*, vol. 5, no. 7, pp. 1843–1853, Jul. 2005.

[16] B. J. Soden and J. R. Lanzante, "An assessment of satellite and radiosonde climatologies of upper-tropospheric water vapor," *J. Climate*, vol. 9, no. 6, pp. 1235–1250, Jun. 1996.

[17] J. Wang and L. Zhang, "Systematic errors in global radiosonde precipitable water data from comparisons with ground-based GPS measurements," *J. Climate*, vol. 21, no. 10, pp. 2218–2238, May 2008.

[18] A. Agustí-Panareda, D. Vasiljevic, A. Beljaars, O. Bock, F. Guichard, M. Nuret, A. Garcia Mendez, E. Andersson, P. Bechtold, A. Fink, H. Hersbach, J. Lafore, J. Ngamini, D. J. Parker, J. Redelsperger, and A. M. Tompkins, "Radiosonde humidity bias correction over the West African region for the special AMMA reanalysis at ECMWF," *Q. J. R. Meteorol. Soc.*, vol. 135, no. 640, pp. 595–617, Apr. 2009.

[19] E. Chung and B. J. Soden, "A satellite-based assessment of upper-tropospheric water vapor measurements during AFWEX," *J. Appl. Meteorol. Clim.*, vol. 48, no. 11, pp. 2284–2294, 2009.

[20] I. Durre, R. S. Vose, and D. B. Wuertz, "Overview of the integrated global radiosonde archive," *J. Climate*, vol. 19, no. 1, pp. 53–68, Jan. 2006.

[21] I. Moradi, S. A. Buehler, and V. O. John, "Comparing upper tropospheric humidity from microwave satellite instruments and IGRA radiosonde data," in *Proc. 11th Spec. Meet. MicroRad/Remote Sens. Environ.*, Washington, DC, Mar. 2010, pp. 146–151.

[22] S.-P. Ho, X. Zhou, Y.-H. Kuo, D. Hunt, and J.-H. Wang, "Global evaluation of radiosonde water vapor systematic biases using GPS radio occultation from COSMIC and ECMWF analysis," *Remote Sens.*, vol. 2, no. 5, pp. 1320–1330, May 2010.

[23] R. W. Saunders, T. J. Hewison, S. J. Stringer, and N. C. Atkinson, "The radiometric characterization of AMSU-B," *IEEE Trans. Microw. Theory Tech.*, vol. 43, no. 4, pp. 760–771, Apr. 1995.

[24] G. Goodrum, K. B. Kidwell, and W. Winston, NOAA KLM User's Guide, Nat. Environ. Satellite, Data, Inf. Serv. (NESDIS), Silver Spring, MD, Tech. Rep. [Online]. Available: http://www.ncdc.noaa.gov/oa/pod-guide/ncdc/docs/klm/index.htm

[25] R. Bonsignori, "The Microwave Humidity Sounder (MHS) in-orbit performance assessment," in *Proc. SPIE—The International Society for Optical Engineering*, Florence, Italy, 2007, vol. 6744, p. 67 440A.

[26] S. A. Buehler, M. Kuvatov, V. O. John, M. Milz, B. J. Soden, D. L. Jackson, and J. Notholt, "An upper tropospheric humidity data set from operational satellite microwave data," *J. Geophys. Res.*, vol. 113, p. D14 110, Jul. 2008.

[27] S. A. Buehler, M. Kuvatov, V. O. John, U. Leiterer, and H. Dier, "Comparison of microwave satellite humidity data and radiosonde profiles: A case study," *J. Geophys. Res.*, vol. 109, p. D13 103, Jul. 2004.

[28] A. Dai, J. Wang, P. W. Thorne, D. E. Parker, L. Haimberger, and X. L. Wang, "A new approach to homogenize daily radiosonde humidity data," *J. Climate*, vol. 24, no. 4, pp. 965–991, Feb. 2011.

[29] S. A. Buehler, P. Eriksson, T. Kuhn, A. von Engeln, and C. Verdes, "ARTS, the atmospheric radiative transfer simulator," *J. Quant. Spectrosc. Radiat. Transf.*, vol. 91, no. 1, pp. 65–93, Feb. 2005.

[30] P. Eriksson, S. Buehler, C. Davis, C. Emde, and O. Lemke, "ARTS, the atmospheric radiative transfer simulator, version 2," *J. Quant. Spectrosc. Radiat. Transfer*, vol. 112, no. 10, pp. 1551–1558, Jul. 2011.

[31] S. A. Buehler and V. O. John, "A simple method to relate microwave radiances to upper tropospheric humidity," *J. Geophys. Res.*, vol. 110, p. D02 110, Jan. 2005.

[32] V. O. John, S. A. Buehler, and N. Courcoux, "A cautionary note on the use of Gaussian statistics in satellite based UTH climatologies," *IEEE Geosci. Remote Sens. Lett.*, vol. 3, no. 1, pp. 130–134, Jan. 2006.

[33] V. O. John, G. Holl, R. P. Allan, S. A. Buehler, D. E. Parker, and B. J. Soden, "Clear-sky biases in satellite infra-red estimates of upper tropospheric humidity and its trends," *J. Geophys. Res.*, vol. 116, p. D14 108, Jul. 2011.

[34] G. Hong, G. Heygster, J. Miao, and K. Kunzi, "Sensitivity of microwave brightness temperatures to hydrometeors in tropical deep convective cloud system at 89–190 GHz channels measurements," *Radio Sci.*, vol. 40, no. RS4003, 2005.

[35] B. Burns, X. Wu, and G. Diak, "Effects of precipitation and cloud ice on brightness temperatures in AMSU moisture channels," *IEEE Trans. Geosci. Remote*, vol. 35, no. 6, pp. 1429–1437, Nov. 1997.

[36] S. A. Buehler, M. Kuvatov, T. R. Sreerekha, V. O. John, B. Rydberg, P. Eriksson, and J. Notholt, "A cloud filtering method for microwave upper tropospheric humidity measurements," *Atmos. Chem. Phys.*, vol. 7, no. 21, pp. 5531–5542, Nov. 2007.

[37] V. O. John and S. A. Buehler, "The impact of ozone lines on AMSU-B radiances," *Geophys. Res. Lett.*, vol. 31, p. L21 108, Nov. 2004.

[38] V. H. Payne, J. S. Delamere, K. E. Cady-Pereira, R. R. Gamache, J. L. Moncet, E. J. Mlawer, and S. A. Clough, "Air-broadened half-widths of the 22- and 183-GHz water-vapor lines," *IEEE Trans. Geosci. Remote*, vol. 46, no. 11, pp. 3601–3617, Nov. 2008.

[39] C. Melsheimer, C. Verdes, S. A. Buehler, C. Emde, P. Eriksson, D. G. Feist, S. Ichizawa, V. O. John, Y. Kasai, G. Kopp, N. Koulev, T. Kuhn, O. Lemke, S. Ochiai, F. Schreier, T. R. Sreerekha, M. Suzuki, C. Takahashi, S. Tsujimaru, and J. Urban, "Intercomparison of general purpose clear sky atmospheric radiative transfer models for the millimeter/submillimeter spectral range," *Radio Sci.*, vol. 40, no. 1, p. RS1 007, Feb. 2005.

[40] B. J. Soden, D. D. Turner, B. M. Lesht, and L. M. Miloshevich, "An analysis of satellite, radiosonde, lidar observations of upper tropospheric water vapor from the atmospheric radiation measurement program," *J. Geophys. Res.*, vol. 109, no. D4, p. D04 105, Feb. 2004.

[41] L. M. Miloshevich, H. Vömel, D. N. Whiteman, B. M. Lesht, F. J. Schmidlin, and F. Russo, "Absolute accuracy of water vapor measurements from six operational radiosonde types launched during AWEX-G and implications for AIRS validation," *J. Geophys. Res.*, vol. 111, no. D9, p. D09S10, Apr. 2006.

[42] J. H. Wang, H. L. Cole, D. J. Carlson, E. R. Miller, K. Beierle, A. Paukkunen, and T. K. Laine, "Corrections of humidity measurement errors from the Vaisala RS80 radiosonde—Application to TOGA COARE data," *J. Atmos. Ocean. Technol.*, vol. 19, no. 7, pp. 981–1002, Jul. 2002.

[43] J. Bian, H. Chen, H. Vmel, Y. Duan, Y. Xuan, and D. L, "Intercomparison of humidity and temperature sensors: GTS1, Vaisala RS80, CFH," *Adv. Atmos. Sci.*, vol. 28, no. 1, pp. 139–146, Jan. 2011.

[44] J. Wang, "Performance of operational radiosonde humidity sensors in direct comparison with a chilled mirror dew-point hygrometer and its climate implication," *Geophys. Res. Lett.*, vol. 30, no. 16, p. 1860, Aug. 2003.

Isaac Moradi received the M.Sc. degree in meteorology from the University of Tehran, Tehran, Iran, in 2003 and the Ph.D. degree in applied climatology from the Khwarizmi University of Tehran, Tehran, in 2006, where he studied atmospheric remote sensing, with an emphasis on retrieving incoming solar radiation from geostationary satellite data.

From 2007 to 2008, he was with the Department of Physical Geography, University of Tehran, and the Department of Space Science, Luleå University of Technology, Kiruna, Sweden, from 2008 to 2011. He is currently an Assistant Research Scientist with the NOAA Cooperative Institute for Climate and Satellites, Earth System Science Interdisciplinary Center (ESSIC), University of Maryland, College Park. His main research interests are retrieving geophysical variables from satellite data, calibration and bias correction for microwave sensors, and solar radiation modeling and data analysis.

Dr. Moradi is a member of the American Geophysical Union and the American Meteorological Society.

Stefan A. Buehler received the M.S. degree in physics from the State University of New York (SUNY), Stony Brook, in 1994 and the Ph.D. degree in physics from the University of Bremen, Bremen, Germany, in 1998.

He is currently a Full Professor with SRT, Luleå University of Technology, Kiruna, Sweden. His research interests include radiative transfer and the remote sensing of water vapor and clouds in the Earth's atmosphere, particularly in the millimeter to submillimeter wavelength range.

Viju O. John received the M.S. degree in physics and the M.S. degree in atmospheric science from the Cochin University of Science and Technology, Cochin, India, in 1998 and 2000, respectively, and the Ph.D. degree in physics from the University of Bremen, Bremen, Germany, in 2005.

He is currently a Senior Scientist with the Met Office Hadley Centre, Exeter, U.K. His research interests include the remote sensing of water vapor in the Earth's atmosphere, intercalibration of satellite sensors, and evaluation climate models using satellite observations.

Anthony Reale, photograph and biography not available at the time of publication.

Ralph R. Ferraro received the B.S. degree in meteorology from Rutgers University, New Brunswick, NJ, in 1980 and the M.S. degree in meteorology from the University of Maryland, College Park, in 1982.

He is currently a Physical Scientist with STAR, National Environmental Satellite, Data, and Information Service, National Oceanic and Atmospheric Administration, College Park, MD, where he is currently the Chief of the Satellite Climate Studies Branch. His research activities include the development of advanced retrieval algorithms for hydrological products with passive microwave sensors.

Mr. Ferraro is also a member of the American Meteorological Society, American Geophysical Union, and the National Weather Association.